Xijiao Dihuang Decoction Alleviates Lung Injury Induced by Sepsis Through Regulating Glycerinpho Spholipid Metabolism Based Lipidomics

Chen Huai yu

　The Affiliated People's Hospital of Fujian University of Traditional Chinese Medicine

Lin Ming rui

　The Affiliated People's Hospital of Fujian University of Traditional Chinese Medicine

Wen Dan

　The Affiliated People's Hospital of Fujian University of Traditional Chinese Medicine

Su Jun feng

　Zhejiang University School of Medicine Second Affiliated Hospital

Yao Jie

　The Affiliated People's Hospital of Fujian University of Traditional Chinese Medicine

Zhu Xue li

　The Affiliated People's Hospital of Fujian University of Traditional Chinese Medicine

Li Wei（✉ sicu_lw@163.com ）

　The Affiliated People's Hospital of Fujian University of Traditional Chinese Medicine

　https://orcid.org/0000-0002-4198-104X

---

1 Xijiao Dihuang Decoction Alleviates Lung Injury induced by Sepsis through

2 Regulating Glycerinpho spholipid Metabolism Based Lipidomics

3 Huaiyu Chen[1†], Mingrui Lin[1 †], Dan Wen[2], Junfeng Su[3], Jie Yao[1], Xueli Zhu[1], Wei Li[1]

4 [1]ICU, [2]Department of Emergency, The People's Hospital of Fujian Traditional Medical

5 University, No. 602, 817 Middle Road, Taijiang District, Fuzhou 350004, Fujian, China

6 [3]Department of General ICU, 2nd Affiliated Hospital, School of Medicine, Zhejiang

7 University, No.1511, Jianghong Road, Binjiang District, Hangzhou(310052), Zhejiang,

8 China

9 †These authors have contributed equally to this work and share first authorship.

10 Corresponding author: Wei Li, E-mail: sicu_lw@163.com

11 **Background and Objective:** To observe the effect of Xijiao Dihuang Decoction

12 (XJDHT) on lung injury of sepsis mice with lipidomic analysis, and explore the

13 underlying mechanisms.

14 **Materials and Methods:** C57BL/6 mice were induced sepsis by lipopolysaccharide

15 (LPS) administration. Animals are pretreated with XJDHT 2 days before LPS

16 regimen, then continue treatment for addition 3 days. Lung tissue are collected for

17 lipidomic analysis by LC/MS/MS. The survival rate is monitor after treatment.

18 **Results:** After treatment with XJDHT, the histological changes of lung of the sepsis

19 mice were relieved. The lipidomic profiles of the lung in sepsis group were evidently

20 disordered when compared to the control group. A total of 40 significantly differential

21 lipids expression between the sepsis-control groups were identified by multivariate

22 statistical analysis. Septic lung injury may result from such lipid disorders, which are

related to fatty acyls metabolism, glycerophospholipid metabolism, phosphosphingolipids metabolism and glycerides metabolism. After XJDHT treatment, the lipidomic profiles of the disorders tend towards alleviated when compared to the sepsis group. Twelve lipid molecules were identified and some glycerophospholipids levels returned close to the normal level.

Conclusion: Glycerophospholipid metabolism may play an important role in the treatment of septic lung injury using XJDHT.

Keywords: Sepsis, XJDHT, LC–MS, mice, lung, lipidomics

Background

Sepsis is a complex disease that usually accompanied with organ dysfunction due to a serious infection [1, 2]. It is associated with high rates of incidence and mortality worldwide. Although using advanced medical technologies，mortality of sepsis has gradually decreased，but it is still not satisfied. About 50% of patients with sepsis develop acute lung injury（ALI） and acute respiratory distress syndrome (ARDS) that increase the mortality up to 34-45% [3-5]. If Chinese traditional medicine and western therapeutics combination therapy can be taken in time, it will reduce the patient stayed in ICU, shorten treatment time, and suppressed disease progression [6].

Li et al. has interpreted sepsis in traditional Chinese medicine as "dysregulating host response to infection" and defined it with syndrome of "Du Re-Zheng" (Toxic-heat), which is the program of "Qi-Feng" (Qi stage) deregulation, follow by "Xue-Feng", subsequently developing "Xue Yu-Zheng" (Blood stasis syndrome). "Du Re-Zheng" is complex and susceptible to further develop acute deficiency syndrome including multiple organ dysfunction syndrome (MODS) [7]. As internal heat toxin is presented

throughout entire sepsis progress [8], clearing heat and detoxifying (Qing Re Jie Du) have been reported to ameliorate ALI induced by sepsis.

Xi Jiao Di Huang Decoction (XJDHT) was first recorded by Sun Simiao in "Beiji Qianjin Yao Fang". It has been used for treatment of Warm Heat from exogenous contraction and blood disease in ancient period. Nowadays, it is used extensively for the treatment of miscellaneous disease in different departments. This is especially the case in acute and severe diseases, such as sepsis. Previous study found that XJDHT suppressed aerobic glycolysis to improve sepsis outcomes through the regulation of TLR4/HIF-1α/PKM2 signaling pathway [9]. Oral administration of XJDHD significantly protected acute liver injury in mice induced by lipopolysaccharide [10].

Recently, correlation between lipid metabolism disorders and various diseases has been received attention. These disorders include cancer, metabolic syndrome, neurological disorder and sepsis. Disruption of lipid metabolism, such as hypertriglyceridemia, decreased high density lipoprotein and low density lipoprotein cholesterol, has been found in septic patients [11]. Similar alteration of lipoprotein may appear in patients of systemic inflammatory response induced by lipopolysaccharide. This phenomenon appears to be linked to disease severity [12].

Lipidomics is a kind of high-throughput technology for the analysis of lipid composition and changes in expression within living organisms to elucidate the mechanisms likely exist [13]. Present study, we will reveal the underlying mechanism of XJDHT on sepsis mice using lipidomic technology and elucidated the potential therapeutic for sepsis.

Methods and Materials

Chemicals

Lipopolysaccharide (LPS, L2630, Escherichia coli serotype O111:B4) were obtained

from Sigma. Ultra performance liquid chromatography (UHPLC) Nexera LC-30A Ultra

High Performance Liquid was from Shimadzu (Kyoto, Japan). Acetonitrile,

Isopropanol, MS-grade methanol, MS-grade acetonitrile, HPLC-grade 2-propanol and

methanol were purchased from Thermo Fisher (MA, USA). HPLC-grade formic acid

and HPLC-grade ammonium formate were purchase from Sigma (MO, USA). 4%

paraformaldehyde solution and Servicebio® Electron microscope fixation was

purchased from Servicebio Company (Wuhan, China).

XJDHT extract preparation

Mixture of crude drugs, 30 g BUBALI CORNU（Shui-Niu -Jiao, the horn of Bubalus

bubalis Linnaeus）, 24 g Rehmannia glutinosa (Gaertn.) DC.（Di-Huang）, 12 g Paeonia

anomala L（Shao-Yao）, and 9 g Paeonia × suffruticosa Andrews Cortex（Mu-Dan-

Pi）, obtained from The People's Hospital of Fujian Traditional Medical University

(Fujian, China), was soaked in 10 volumes water for 0.5 h and refluxed for 2 h. Liquid

extract was saved and residue was refluxed with 8 volumes water for addition 1 h.

Combined liquid was filtered through 0.2 um filter and the filtrations were concentrated

in a vacuum evaporator to produce XJDHT extract with concentration of 3 g/ml.

XJDHT extract was aliquoted and stored at -80°C.

UHPLC fingerprint analysis of the XJDHT

An ACQUITY UHPLC I-Class system coupled with a Xevo XS quadrupole time of

flight mass spectrometer (Waters, Milford, MA, USA) was used for characterization of

chemical components in XJDHT formulae fingerprint. Chromatographic separation

was carried out at 40 °C on a Waters CORTECS C18 column (2.1 mm × 100 mm; 1.6

94 μm), with 0.1% of formic acid in water as mobile phase A and acetonitrile as mobile

95 phase B. Gradient elution was performed as follows: 5%–5% B for 0–0.5 min, 5%–15%

96 B for 0.5–2.5 min, 15%–35% B for 2.5–4.5 min, 35%–35% B for 4.5–5.0 min, 35%–

97 53% B for 4.5–6.4 min, and 53%–80% B at 6.5–7.5 min. The flow rate was 0.25

98 mL/min. The mass-spectrometry conditions were optimized as follows: ESI negative

99 mode, desolvent gas temperature, 500 °C; capillary voltage, 2.5 kV; source temperature,

100 150 °C; desolvent gas flow, 800 L/h; and cone gas flow, 50 L/h. The MS scan range

101 was m/z 50–1000, and the collision energy was set at 20-50 eV.

102 **Animals**

103 143 female C57BL/6 mice, age 6-8 weeks, were purchase from Shanghai SLAC

104 Laboratory Animal Co., Ltd (Animal licenses: SCXK（Shanghai）2017-0005, China).

105 Animals were housed in the facility with temperature 20-22°C and constant humidity

106 45-60% under 12/12 hours light/dark cycle. Food and tap water were provided ad

107 libitum.

108 **Animal study**

109 Animals were habituated for 7 days before experiments, then randomly divided into

110 three groups: control group (CP group, n=20), model group (SP group, n=62), XJDHT

111 group (XP group, n=61). For sepsis model, animals were either intraperitoneally (i.p.)

112 injected LPS at the dose of 25 mg/kg (SP group and XP group) or saline (CP group).

113 XP group animals were pretreated with 9.45g/kg XJDHT extract gavage (g.v.) twice

114 daily (BID) for 2 days before LPS challenge, following continue treatment for

115 additional 3 days, while animals of SP group and CP group were received same volume

of saline during same period. 22 animals from SP and 21animals from XP group were monitored for survival rate. 10 animals from each group were anesthetized and sacrificed by decapitation after 5-days treatment, lung tissue was harvested for further analysis.

Histology

Optical microscopy observation

Animals were sacrificed, lung tissue were removed and fixed in 4% paraformaldehyde (PFA) solution overnight at 4 °C. 10 μm tissue sections were sliced with cryostat and stained with hematoxylin and eosin (H&E). The pictures were captured under microscope (Nikon Eclipse E100, Japan).

Transmission electron microscopy (TEM) observation

Less than 1 mm × 1 mm × 1 mm lung tissue were collected and fixed with Servicebio® Electron microscope fixation，then rinse with 0.1M phosphate buffer Pb (pH7.4) and post-fix monolayer in 1% osmic acid-0.1M phosphate buffer Pb (pH7.4) at room temperature (20 °C) for 2 hours and dehydrated with a graded series of alcohol. And then the tissue was permeated overnight with a 1:1 mixture of acetone and 812 embedding agents and polymerized in a 60°C oven overnight. Ultrathin sections were processed and Morphology was observed by transmission electron microscopy (HT7700, HITACHI, Japan).

Tissue lipid extraction

Lung tissue were removed, quickly cryopreserved in liquid nitrogen, and stored at -80°C for lipomics analysis. Lipids were extracted according to MTBE method [14].

138   Briefly, tissues were cut in small pieces, spiked with appropriate amount of internal

139   lipid standards, then homogenized with 440 µL water/methanol (5:6) solution. 800 µL

140   MTBE was added, sonicated for 20min at 4°C with ultrasound, and incubated for 30

141   min at room temperature. The upper layer was harvested after centrifugation with 14000

142   g for 15min at 10°C and dried under nitrogen.

143   **LC-MS/MS lipid analysis**

144   The lipid was resuspended in 200 µL 90% isopropanol/acetonitrile, centrifuged at

145   14000 g for 15 min, and collected with liquid layer. 3 µL of sample was injected for

146   lipid panel analysis with CSH C18 column (1.7 μm, 2.1 mm × 100 mm) using LC-

147   MS/MS (UHPLC Nexera LC-30A, SHIMADZU). Reverse phase chromatography

148   mode was selected, solvent A was comprised of 0.1% formic acid and 0.1mM

149   ammonium formate in acetonitrile–water (6:4，v/v) and solvent B was comprised of

150   0.1% formic acid and 0.1mM ammonium formate in acetonitrile–isopropanol (1:9, v/v).

151   The initial mobile phase was 30% solvent B at a flow rate of 300 µL/min. It was held

152   for 2 min, and then linearly increased to 100% solvent B in 23 min, followed by

153   equilibrating at 5% solvent B for 10 min. Mass spectra was acquired by Q-Exactive

154   Plus in positive and negative mode, respectively. ESI parameters were optimized and

155   preset for all measurements as follows: Source temperature was set at 300 °C, Capillary

156   Temp was set at 350 °C, the ion spray voltage was set at 3000V, S-Lens RF Level was

157   set at 50% and the scan range of the instruments was set at m/z 200–1800. Lipid

158   compounds were identified using LipidSearch™ software, which contains more than

159   30 lipid classes and more than 1,500,000 fragment ions in the database. Both mass

160   tolerance for precursor and fragment were set to 5 ppm.

161   **Statistics**

162   Survival rate were analyzed using SPSS 19.0 statistical software (SPSS, Chicago, USA).

163   One-way ANOVA followed by the Bartlett's test was performed using GraphPad Prism

164   6.01 (Graphpad Software, Inc, USA). $p < 0.05$ was considered statistically significant.

165   **Results**

166   **Chemical components of XJDHT formulae fingerprint**

167   Total ion chromatogram fingerprint was shown in Figure 1, the qualitative compounds

168   list at Table S1.

169   **XJDHT treatment increases survival rate in murine sepsis model**

170   LPS-induced lethal sepsis has been well studied [15]. Here, we investigated whether

171   classic herb formula XJDHT was able to block LPS-induced sepsis. First, we evaluated

172   the effect of XJDHT treatment on LPS-induced animal mortality. Pretreated animals

173   with XJDHT (9.45g/kg, BID, g.v.) for 5 days has showed extending animal survival

174   time in LPS-induced lethal model (Figure. 2). Animals in XJDHT treatment group

175   significantly increased median survival time with 45 hours in SP group (n=22) vs 60

176   hours in XP group (n=21) (P = 0.045), indicating the protective effect of XJDHT in

177   serious inflammatory-death.

178   **XJDHT treatment reversed LPS-induced lung inflammation and relieve**

179   **mitochondrial swelling**

180   Many studies have showed that high dose of LPS regimen induced systemic sepsis,

181   subsequently lung function was affected [16]. We determined whether XJDHT

182 treatment was able to prevent lung injury induced by LPS. Mice were pretreated with

183 9.45g/kg/d XJDHT for 2 days before LPS challenge, following additional 3 days

184 XJDHT treatment and lung tissues were sliced for H&E staining and Transmission

185 electron microscopy (TEM) observation. Histologic study showed pathological

186 changes in lung tissue after LPS challenge that had been eliminated by XJDHT

187 treatment (Figure. 3). As shown in Figure 3, LPS (25 mg/kg, i.p.) administration

188 induced lung alveolar walls damage, initiated lymphocyte infiltration (Figure. 3B-B1),

189 severe mitochondrial swelling (Figure.3E), and XJDHT treatment restored lung

190 alveolar wall structure and reduced lymphocyte infiltration (Figure. 3C-C1) and relieve

191 mitochondrial swelling (Figure.3F). Our data suggested that XJDHT treatment

192 profound reversed LPS-induced lung inflammation and relieve mitochondrial swelling.

193 **LPS disrupted lipid homeostasis in murine lung tissue**

194 According to the international lipid classification and Nomenclature Committee, lipid

195 compounds are divided into eight categories and their subtypes based on the polarity

196 head and saturation degree or length of carbon chain [17]. So far, 1251 lipid species and

197 30 lipid classes have been identified (Figure.S1).

198 First, to establish methodology for lipidomic analysis, Quality control（QC）samples

199 were run with UHPLC and lipid species were analyzed by Lipid Search software.

200 The comparison base peak chromatograms (BPC) spectra of QC samples in positive-

201 and negative-ion mode, as shown in Supplement Figure S2 A-B. The peak response

202 intensity and retention time of QC samples were basically overlapped and correlation

203 coefficients of QC samples are all above 0.9 assessed by pearson correlation analysis

204 (Supplement Figure S2C), and the R^2Y and Q2 evaluation parameters of OPLS-DA are

205 0.812 and 0.998 respectively (Supplement Figure S2D), suggesting that the

206 methodology is repeatable and reliable. Subsequently, we analyzed Lipid composition

207 in lung tissues of control group and LPS group and found 5 major lipid classes,

208 triglyceride(TG), phosphatidylcholine (PC), phosphatidylethanolamine (PE),

209 sphingomyelin(SM), phosphatidylserine (PS), present in both groups (Figure 4A-B).

210 However, Figure 4C shows the dynamic distribution range of lipid content. The highest

211 lipid molecules is PC (16:0/16:0)+HCOO in both group. The lowest lipid molecules are

212 Cer (d18:0+pO/34:3)+HCOO in control group and Cer (d60:5+hO)+HCOO in sepsis

213 group. Figure 4D shows the statistical results of the number of lipid subclasses (lipid

214 classes) identified in positive and negative ion modes and the number of lipid molecules

215 identified in each category.

216 **LPS-induced lung injury was mediated by glycerophospholipid metabolism**

217 Univariate analysis was performed for the different analyses of all detected lipid

218 molecules and the analysis results were displayed in the form of a volcano map (Figure

219 5A). The lipid molecules with FC > 1.5 or FC < 0.67, P value < 0.05 are represented by

220 different colors. FC > 1.5 or FC < 0.67 metabolites in the control and sepsis groups

221 were demonstrated in Figure 5B. Differential lipid molecules analysis was also used to

222 verify the significant difference in lung lipids. The difference was considered to be

223 significant (VIP>1, P < 0.05). The 40 lipids (Supplemental table S2) include 5 Fatty

224 acyls, 22 Glycerophospholipid, 4 Phosphosphingolipids, 9 Glycerides. As shown in

225   Supplemental table S2, compared with the control group, there were 25 up-regulated

226   and 15 down-regulated in the sepsis group.

227   Fatty acyls: 1 acetyl CoA carboxylase （AcCA） showed an upward trend; 4

228   Diacylglycerols（DGs）showed an upward trend except DG(16:0/16:1)+NH4.

229   Glycerophospholipid: 3 Lysophosphotidylserines（LPSs）showed an upward trend.

230   Among the 8 PCs, except PC (14:0 / 14:0) + HCOO, PC (16:1 / 14:0) + HCOO showed

231   a downward trend, 3 PE showed a downward trend, 4 PGs showed an upward trend

232   except PG (16:0 / 16:1) - H, 1 PI showed an upward trend, and among the 3 PSs showed

233   a downward trend except PS (16:0 / 22:6) + H.

234   Phosphosphingolipids: 4SMs were up-regulated.

235   Glycerides: There were 6 TGs showed a downward trend, 3TGs showed an upward

236   trend. The results showed that the lipid metabolism of sepsis mice induced by

237   lipopolysaccharide was abnormal.

238   In order to evaluate the plausibility of different lipids, and display the relationship

239   between samples and the differences of lipids expression patterns in different samples

240   more comprehensively and visually, hierarchical clustering of each sample was

241   undertaken, and the qualitative expression quantity was used to analyze the difference

242   of lung lipid, which was helpful for accurate lipid screening. Figure 5C showed the

243   expression of different lipid molecules in sepsis and control group. The graph can

244   clearly distinguish the sepsis group from the control group, that is, the same group of

245   samples can appear in the same cluster through clustering. At the same time, the lipids

246   with similar expression pattern can also be seen clearly. The lipids in the same cluster

247 may be in a relatively close reaction step in the process of metabolism.

248 Our analyses suggested extensive changes in the lung lipidome of mice under

249 polysaccharide intervention. Therefore, in order to elucidate possible broad

250 organization principles of co-regulation of lipid species, a pairwise correlation analysis

251 for the lipid species was carried out. And then a wide range of positively and negatively

252 correlated lipid species were found (Figure 6A). Further, in order to reveal the

253 coregulatory relationship of lipids more intuitively. The chord diagrams showed lipid

254 molecular pairs with correlation coefficient $|R|= 0.8$ and $P < 0.05$. We found that some

255 lipid classes may prefer to correlate with inter-class (e.g., TG), whereas other classes

256 (e.g., PC, PE, PG, LPS, PS, SM, DG in the nucleus) showed both intra- and inter-class

257 correlations (Figure 6B). Of note, phosphatidylinositol (PI) showed intraclass

258 correlations.

259 **XJDHT treatment corrected LPS-disrupted lipid homeostasis**

260 As previous shown that LPS modulated lipid changes in lung tissues, we determined

261 whether XJDHT treatment alleviated lung injury through regulating lipid metabolism.

262 After 5 days treatment of XJDHT, the changes of all lipids induced by LPS had been

263 toward to normal levels (Figure 7). Notably, 9 of 12 lipids are glycerophospholipid

264 family, including PG (18:1/18:2)-H，LPS (20:4)+H，LPS (22:4)+H，LPS (22:6)+H,

265 PC (16:1/16:1)+HCOO, PC (18:1/22:6)+HCOO, PC (18:2/22:6)+HCOO, PC (34:3)+H,

266 PS (16:0/22:6)+H. Other significant changes were founded in Fatty acyls DG

267 (16:0/22:6)+NH4, Phosphosphingolipids SM (d24:0/18:2)+HCOO and Glycerides TG

268   (18:0/16:0/16:0)+NH4. Together, our data indicated that lipid metabolism was involved

269   in XJDHT treatment in lung sepsis.

270   **Discussion**

271   In this study, XJDHT was able to improve inflammatory changes and relieve

272   mitochondrial swelling of lung tissue and reduce mortality rate of 15 hours in septic

273   mice. However, it is still unclear whether protective effect of XJDHT can be achieved

274   by regulating the changes of Lipid spectrum. Therefore, the lung tissue of mice was

275   characterized from lipid perspective and the effect of XJDHT on sepsis lipid

276   composition was further uncovered. The composition of lipid components was

277   observed varies greatly in control, LPS-induced lung sepsis and XJDHT treatment

278   groups.

279   To the best of our knowledge, we here reported the lipidomic study of the

280   administration of XJDHT to mice with sepsis to identify the lipid profile that could be

281   useful for disease diagnosis or prediction, and that explored underlying pathogenesis of

282   XJDHT for the first time. The glycerophospholipid metabolism and arachidonic acid

283   (AA) metabolism may play crucial roles in the treatment of sepsis with XJDHT that is

284   a clear strength of this study.

285   Glycerophospholipid metabolism contributes importantly to septic lung injury induced

286   by lipopolysaccharide. In normal lung tissue, there is a barrier that selectively passes

287   through fluid and solute. This barrier is composed of monolayer endothelial cells, which

288   are connected by adherent bodies and tightly connected plasma membrane structures

289   [5, 18]. Alveolar epithelium is a very tight barrier formed by flat alveolar type I (ATI)

cells and cubic alveolar type II (ATII) cells. It allows the diffusion of carbon dioxide

and oxygen, but limits the passage of small solutes [19]. In acute respiratory distress

syndrome induced by sepsis, pulmonary interstitial edema is often caused by increased

permeability of fluid and protein through the pulmonary endothelium. The normal tight

barrier properties of alveolar epithelium are usually impaired when edematous fluid is

transferred to the alveoli [20-22]. Glycerophosphatide is one of the most abundant

phospholipids in the body. It is one of the important components of the cell membrane,

and participates in the protein recognition and signal transduction. There are 7 major

classes of glycerophospholipids, including PC, PE, PS, PI, LPE, LPS and PG [23].

Among those, PC and PE, are accounted for more than half of the total phospholipids

in eukaryotic cells. Proper phospholipid composition is the key structure and function

to establish and maintain membrane integrity [24, 25]. Abnormal phospholipid

composition is accompanied by loss of membrane structural integrity [26].

Evidence indicated that PC is an essential phospholipid in mammalian cells and tissues

and is made in all nucleated cells via the choline pathway [27]. PC as a kind of

phospholipid is an essential lipid composition of lung surfactant, which might play the

role in anti-inflammatory effects [27]. Previous studies have demonstrated that the

decrease of PC levels on plasma membrane of liver in the liver injury model and then

the hepatocyte membrane might become permeable and the end result was that liver

failure happened [28]. As showed in Figure 7, the expression levels (mean) of PC

(16:1/16:1) + HCOO, PC (18:1/22:6) + HCOO, PC (18:2/22:6) + HCOO, PC (34:3) +

H were significantly downregulated in the lung of septic mice induced by

lipopolysaccharide and restored after XJDHT treatment. A previous study showed that

XJDHT also has anti-inflammatory effects through decreasing the level of IL-1β and

IL-6 [9, 29]. Therefore, the interference of XJDHT with PC may change the ability of

the body to resist inflammation.

LPS are involved in the activities of Toll-like receptors (TLRs) [30] and G protein

coupled receptors (GPCRs) [31-33]. Such activities are involved in the occurrence and

developmental process of sepsis [34, 35]. LPSs have emerged in regulating macrophage

activation and enhances their clearance of apoptotic cells [36]. As to lipid molecules,

we know that the expression of LPS (20:4) + H, LPS (22:4) + H, LPS (22:6) + H in the

lung tissue of sepsis mice decreased significantly, but increased significantly after

XJDHT intervention (Figure 7). And abnormally high expression of PG (18:1/18:2) -

H，PS (16:0/22:6) + H in septic mice induced by lipopolysaccharide were resolved.

Therefore, LPS (20:4) + H, LPS (22:4) + H, LPS (22:6) + H, PC (16:1/16:1) + HCOO,

PC (18:1/22:6) + HCOO, PC (18:2/22:6) + HCOO, PC (34:3) + H, PG (18:1/18:2) – H,

PS (16:0/22:6) + H may be the targets of XJDHT.

Conclusion In this study, the UHPLC high resolution mass spectrometry based on the

strategy of absolute quantitative lipomics was used to detect the lipid profile of lung

tissue of septic mice treated with XJDHT, and further elucidated the possible

mechanism of sepsis induced by lipopolysaccharide. Based on the repeatability of

quality control results, the method is considered to be reliable. Multivariate analysis

showed that XJDHT could treat lipopolysaccharide induced sepsis associated lung

injury, which was consistent with pathological results. When the lipid distribution in

lung tissue of mice in control group and lipopolysaccharide intervention group was compared, significant changes of 40 kinds of lipid levels were observed. After treatment with XJDHT, the expression of 12 kinds of lipids including 9 kinds of glycerophosphatides showed significant remission. Therefore, XJDHT may regulate the metabolism of glycerophosphatides to treat septic lung injury induced by lipopolysaccharide.

Abbreviations

XJDHT: Xijiao Dihuang Decoction; ALI : Acute lung injury; ARDS: Acute respiratory distress syndrome; MODS: Multiple organ dysfunction syndrome; LPS: Lipopolysaccharide; UHPLC: Ultra performance liquid chromatography; CP group: Control group; SP group: Model group; XP group: XJDHT group; BID: Twice daily; PFA: Paraformaldehyde; H&E: Hematoxylin and eosin; TEM: Transmission electron microscopy; QC: Quality control; BPC: Base peak chromatograms; TG: Triglyceride; PC: Phosphatidylcholine; PE: Phosphatidylethanolamine; SM: Sphingomyelin; PS: Phosphatidylserine; AcCA: Acetyl CoA carboxylase; DGs: Diacylglycerols; LPSs: Lysophosphotidylserines; AA: Arachidonic acid; ATI: Alveolar type I; ATII: Alveolar type II; TLRs: Toll-like receptors; GPCRs: G protein coupled receptors.

Acknowledgement

356 performing the XJDHT formulae fingerprint analysis experiments.

357 **Author contribution:** LW conceived and designed the experiments. CHY and LMR

358 performed the experiments and wrote the manuscript. WD revised the paper. YJ

359 performed the experiments. SJF and ZXL performed the analysis following

360 constructive discussions. All authors read and approved the final version of the

361 manuscript.

367 **Availability of data and materials**

368 The datasets used and/or analyzed during the current study are available from the

369 corresponding author upon reasonable request.

370 **Ethics approval and consent to participate**

371 All procedures in this study were strictly performed according to the Guidelines of the

372 Animal Care and Use Committee of Fujian Academy of Chinese Medical Sciences.

373 (Ethical batch number：FJATCM-IAEC2019058).

374 **Consent for publication**

375 All of authors consent to publication of this work in Chinese Medicine.

376 **Competing interests**

377 The authors declare that they have no competing interests.

References

1. Mervyn Singer, Clifford S Deutschman, Christopher Warren Seymour, et al. The Third International Consensus Definitions for Sepsis and Septic Shock (Sepsis-3). Jama. 2016; 315(8): 801-810.

2. Kristina E Rudd, Sarah Charlotte Johnson, Kareha M Agesa, et al. Global, regional, and national sepsis incidence and mortality, 1990-2017: analysis for the Global Burden of Disease Study. Lancet. 2020; 395(10219): 200-211.

3. Alpha A Fowler 3rd, Jonathon D Truwit, R Duncan Hite, et al. Effect of Vitamin C Infusion on Organ Failure and Biomarkers of Inflammation and Vascular Injury in Patients With Sepsis and Severe Acute Respiratory Failure: The CITRIS-ALI Randomized Clinical Trial. Jama. 2019; 322(13): 1261-1270.

4. Gordon, Rubenfeld, Ellen, et al. Incidence and outcomes of acute lung injury. New England Journal of Medicine. 2005; 20;353(16): 1685-1693.

5. Matthay MA, Zemans RL, Zimmerman GA, et al. Acute respiratory distress syndrome. Nat Rev Dis Primers. 2019; 5(1):18.

6. Wang Y, Zhang Y, Jiang R. Early traditional Chinese medicine bundle therapy for the prevention of sepsis acute gastrointestinal injury in elderly patients with severe sepsis. Scientific Reports. 2017; 7(1): 46015.

7. Li Z, Li Y. Distinguishing the "Wei Qi Ying Xue" syndrome differentiation from the "three certificates and three methods" to the diagnosis of sepsis. Chinese Critical Care Medicine. 2019; 31(2): 135-8.

8. Sun D, Yang Y, Liang Q. Research Progress of Chinese Medicine Treating Acute

Lung Injury Caused by Sepsis. Liaoning Journal of Traditional Chinese Medicine. 2019; 046(005): 1108-10.

9. Lu J, Zhang L, Cheng L, et al. Xijiao Dihuang decoction improves prognosis of sepsis via inhibition of aerobic glycolysis. Biomedicine & Pharmacotherapy. 2020; 129:110501.

10. Liu Y, Zhu L, Li R, et al. Xijiao Dihuang Decoction and Rehmannia glutinosa Libosch. protect mice against lipopolysaccharide and tumor necrosis factor alpha-induced acute liver failure. Chinese journal of integrative medicine. 2019; 25(6):446-453.

11. Dieter M, Swinnen JV, Frank V, et al. Contribution of Circulating Lipids to the Improved Outcome of Critical Illness by Glycemic Control with Intensive Insulin Therapy. Journal of Clinical Endocrinology & Metabolism. 2004; 89(1): 219-226.

12. Levels JHM, Lemaire LCJM, van den Ende AE, et al. Lipid composition and lipopolysaccharide binding capacity of lipoproteins in plasma and lymph of patients with systemic inflammatory response syndrome and multiple organ failure. Crit Care Med. 2003; 31(6): 1647-1653.

13. Zhao Y, Miao H, Cheng X, et al. Lipidomics: Novel insight into the biochemical mechanism of lipid metabolism and dysregulation-associated disease. Chemico-biological interactions. 2015; 240:220-238.

14. Matyash V, Liebisch G, Kurzchalia TV, et al. Lipid extraction by methyl-tert-butyl ether for high-throughput lipidomics. Journal of lipid research. 2008; 49(5): 1137-1146.

422   15. Rathkey JK, Junjie Z, Zhonghua L, et al. Chemical disruption of the pyroptotic

423   pore-forming protein gasdermin D inhibits inflammatory cell death and sepsis.

424   Science Immunology. 2018;   3(26): eaat2738.

425   16. Wang H-r, Guo X-y, Liu X-y, et al. Down-regulation of lncRNA CASC9

426   aggravates sepsis-induced acute lung injury by regulating miR-195-5p/PDK4 axis.

427   Inflammation Research. 2020; 69(6): 559-568.

428   17. Fahy E, Subramaniam S, Murphy RC, et al.Update of the LIPID MAPS

429   comprehensive classification system for lipids. J Lipid Res. 2009; 50 Suppl(Suppl):

430   S9-14.

431   18. Bhattacharya J, Matthay M. Regulation and repair of the alveolar-capillary barrier

432   in acute lung injury. Annual review of physiology. 2013; 75: 593-615.

433   19. Matthay MA. Resolution of pulmonary edema. Thirty years of progress. American

434   Journal of Respiratory and Critical Care Medicine. 2014; 189(11): 1301-1308.

435   20. Bachofen M, Weibel ER. Structural alterations of lung parenchyma in the adult

436   respiratory distress syndrome. Clinics in Chest Medicine. 1982; 3(1): 35.

437   21. Bhattacharya J, Matthay MA. Regulation and Repair of the Alveolar-Capillary

438   Barrier in Acute Lung Injury. Annual Review of Physiology. 2013; 75(1): 593-615.

439   22. Matthay MA, Ware LB, Zimmerman GA. The acute respiratory distress syndrome.

440   Journal of Clinical Investigation. 2012; 122(8): 2731.

441   23. Fein A, Grossman RF, Jones JG, et al. The value of edema fluid protein

442   measurement in patients with pulmonary edema. The American Journal of

443   Medicine. 1979; 67(1): 32-38.

444   24. Dennis EA, Cao J, Hsu YH, et al. Phospholipase A2 enzymes: physical structure,

445   biological function, disease implication, chemical inhibition, and therapeutic

446   intervention. Chemical Reviews. 2011; 111(10): 6130-6185.

447   25. Schaloske RH, Dennis EA. The phospholipase A2 superfamily and its group

448   numbering system. BBA - Molecular and Cell Biology of Lipids. 2006;

449   1761(11):1246-1259.

450   26. Tzu-Ling Chen, Hung-Chi Yang, Cheng-Yu Hung, et al. Impaired embryonic

451   development in glucose-6-phosphate dehydrogenase-deficient Caenorhabditis

452   elegans due to abnormal redox homeostasis induced activation of calcium-

453   independent phospholipase and alteration of glycerophospholipid metabolism.

454   Cell Death & Disease. 2017; 12;8(1): e2545.

455   27. Li Z, Vance DE. Phosphatidylcholine and choline homeostasis. Journal of Lipid

456   Research. 2008; 49(6): 1187.

457   28. Li Z, Agellon LB, Allen TM, et al.The ratio of phosphatidylcholine to

458   phosphatidylethanolamine influences membrane integrity and steatohepatitis. Cell

459   Metab. 2006; 3(5): 321-331.

460   29. Xiaojun F, Xu Z, Qi W, et al. Xijiao Dihuang Decoction Alleviates Ischemic Brain

461   Injury in MCAO Rats by Regulating Inflammation, Neurogenesis, and

462   Angiogenesis. Evidence Based Complementary & Alternative Medicine. 2018: 1-

463   12.

464   30. van der Kleij D, Latz E, Brouwers JF, et al. A novel host-parasite lipid cross-talk.

465   Schistosomal lyso-phosphatidylserine activates toll-like receptor 2 and affects

466   immune polarization. J Biol Chem. 2002; 277(50): 48122-48129.

467   31. Inoue A, Ishiguro J, Kitamura H, et al. TGFα shedding assay: an accurate and

468   versatile method for detecting GPCR activation. Nat Methods. 2012; 9(10): 1021-

469   1029.

470   32. Makide K, Uwamizu A, Shinjo Y, et al.Novel lysophosphoplipid receptors: their

471   structure and function. J Lipid Res. 2014; 55(10):1986-1995.

472   33. Sugita K, Yamamura C, Tabata K, et al. Expression of orphan G-protein coupled

473   receptor GPR174 in CHO cells induced morphological changes and proliferation

474   delay via increasing intracellular cAMP. Biochem Biophys Res Commun. 2013;

475   430(1): 190-195.

476   34. Tarek M El-Achkar, Xiaoping Huang, Zoya Plotkin, et al. Sepsis induces changes

477   in the expression and distribution of Toll-like receptor 4 in the rat kidney.

478   American Journal of Physiology Renal Physiology. 2006; 290(5): F1034.

479   35. Wu TT, Chen TL, Loon WS, et al. Lipopolysaccharide stimulates syntheses of toll-

480   like receptor 2 and surfactant protein-A in human alveolar epithelial A549 cells

481   through upregulating phosphorylation of MEK1 and ERK1/2 and sequential

482   activation of NF-κB. Cytokine. 2011; 55(1):40-47.

483   36. Frasch SC, Bratton DL. Emerging roles for lysophosphatidylserine in resolution

484   of inflammation. Prog Lipid Res. 2012; 51(3): 199-207.

485

486   **Figure Legends**

487   Figure 1. Total ion chromatogram fingerprint of XJDHT formulae.

Figure 2. Survival curves were analyzed by log-rank (Mantel-Cox) test demonstrating an increase in median survival of 15 hours in the XJDHT treatment group (P<0.05).

Figure 3. Histopathological changes of lung. (A-A1): Normal control group, no obvious abnormality in the structure of bronchus, the alveolar wall was composed of a single layer of epithelium, and the structure was clear; there was no obvious abnormality in the interstitium including connective tissue and blood vessels in the lung, and there was no obvious inflammatory change. (B-B1):Sepsis group, Mild *to* moderate alveolar wall thickening，black arrow indicates inflammatory cell infiltrates. No other obvious abnormalities were observed in the tissue. (C-C1): XJDHT treatment group, no obvious abnormality of bronchial structure in visual field, clear alveolar structure, No obvious inflammatory infiltration. (H&E × 200), Original magnification; × 400. Scale bar represents 50 μm. Normal control group (D): Mild mitochondrial swelling (black arrow). Sepsis group(E)：Severe mitochondrial swelling (black arrow). XJDHT treatment group, Moderate mitochondrial swelling (black arrow).

Figure 4. (A-B): The composition of lipid classes in control group and sepsis group; C: The dynamic distribution range of lipid content of different groups; D: Lipid subgroup and lipid molecule count were based on the International Lipid Classification and Nomenclature Committee. Abscissa indicates lipid class was detected, Ordinate indicates lipid species.

Figure 5. Principal component analysis of population samples in mice lung based on UHPLC-Orbitrap MS. (A) volcano plot of Sepsis-Control, red point represents the different lipids (FC > 2.0, P-value < 0.05); (B) Fold-change analysis of the different

510   lipids between Sepsis-Control (CP-Control group, SP-sepsis group); (C) Clustering

511   heat map of the lipids.

512   Figure 6. Lipomics analysis of the lung samples in septic mice. (A) Correlation

513   clustering heat map of the lipids. Red means positive correlation, blue means negative

514   correlation, color depth is related to the absolute value of correlation coefficient. The

515   depth of color is proportional to the level of correlation coefficient. (B) Chord diagram

516   of correlated lipid pairs in the lung of septic mice. The significant difference of lipid

517   molecules was showed by a node around the circle plot and the lipid subclasses were

518   demonstrated by color coded. The color lines show the intra-class correlation, and the

519   lines are the same color with the subclass. Dark gray lines represent interclass

520   correlation.

521   Figure 7 Differential expression levels (mean) of 12 differential lipids in different

522   groups. A comparison of the relative intensities of the potential biomarkers in the

523   control, sepsis, XJDHT groups. *$P < 0.05$ vs control group; **$P < 0.01$ vs control group;

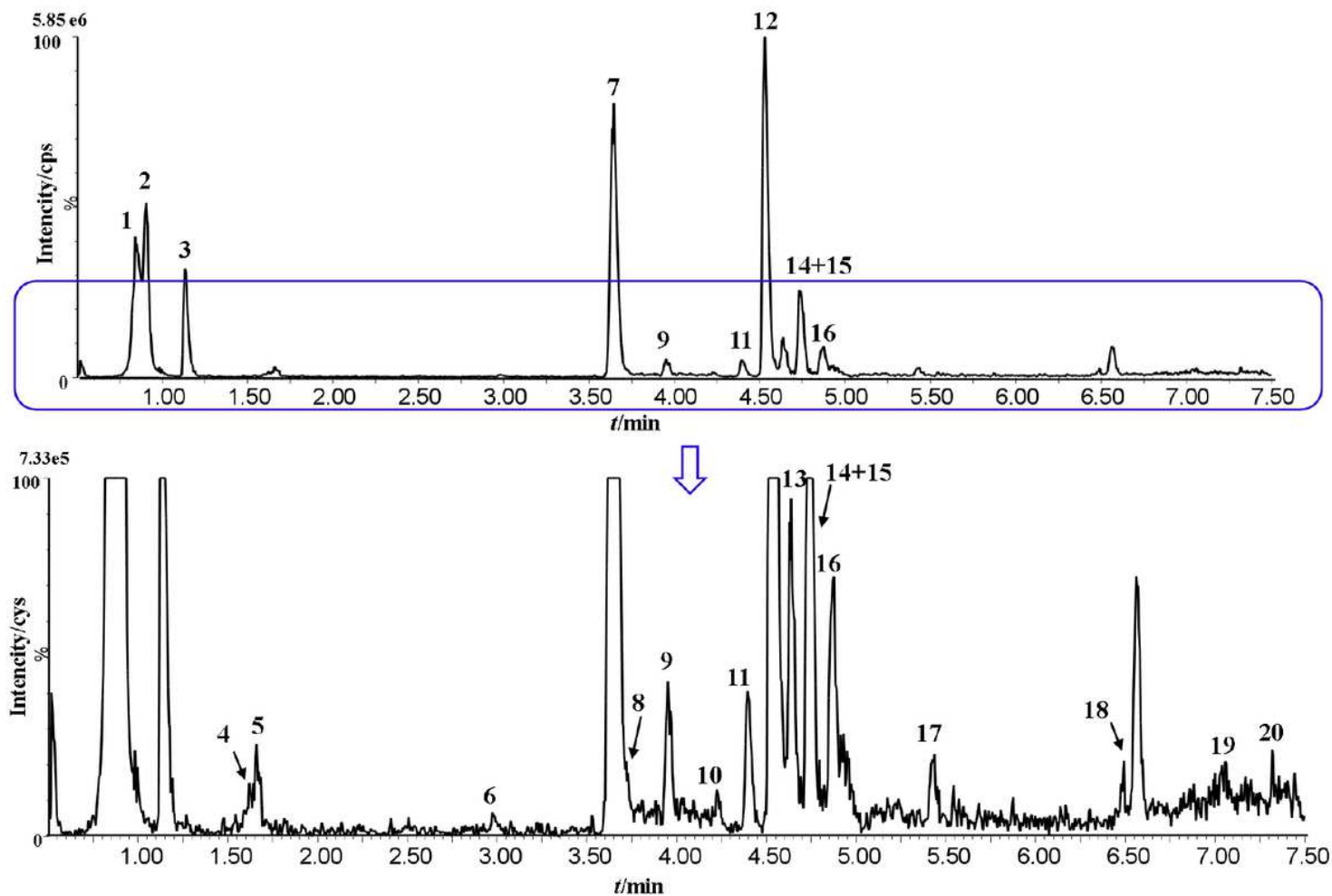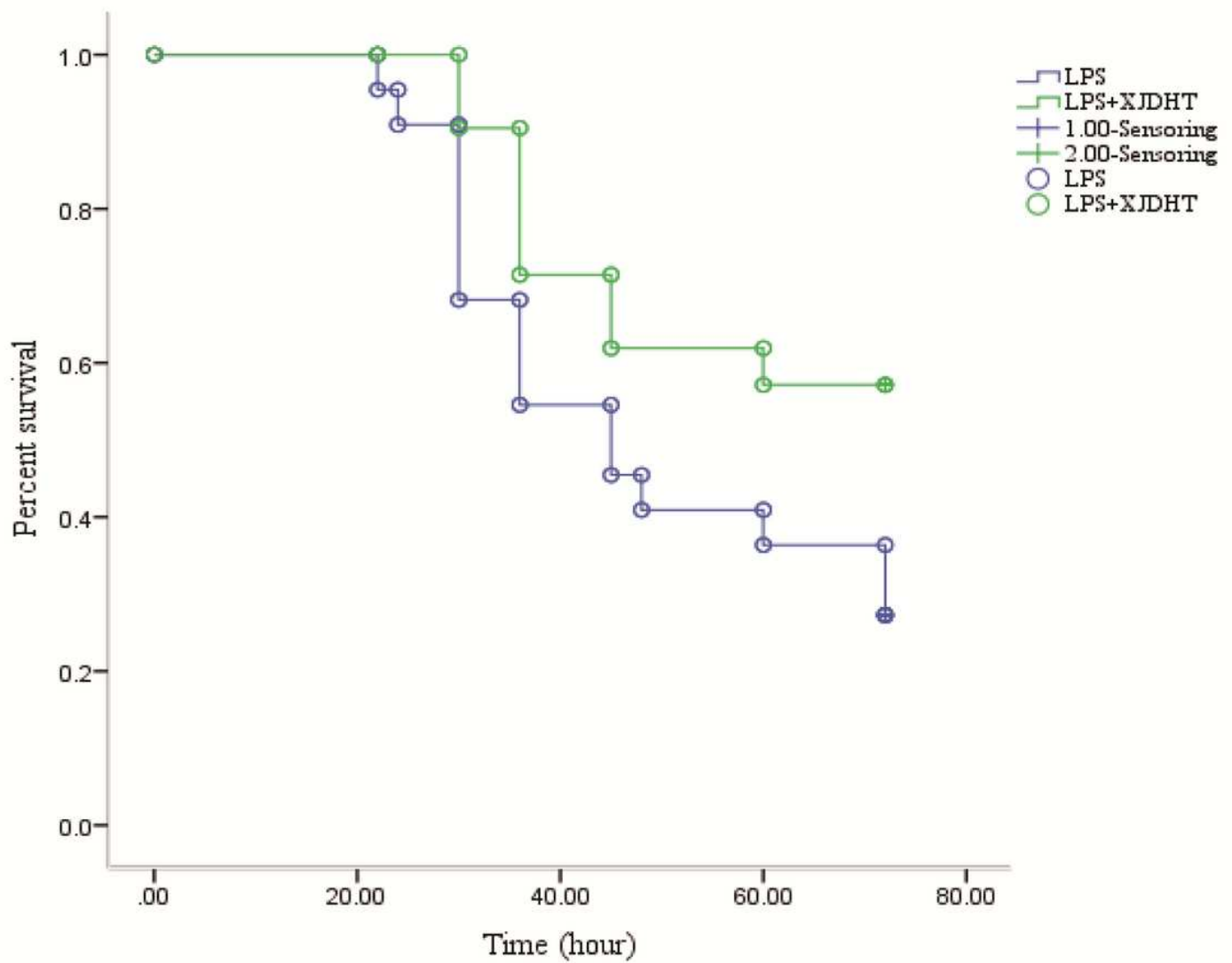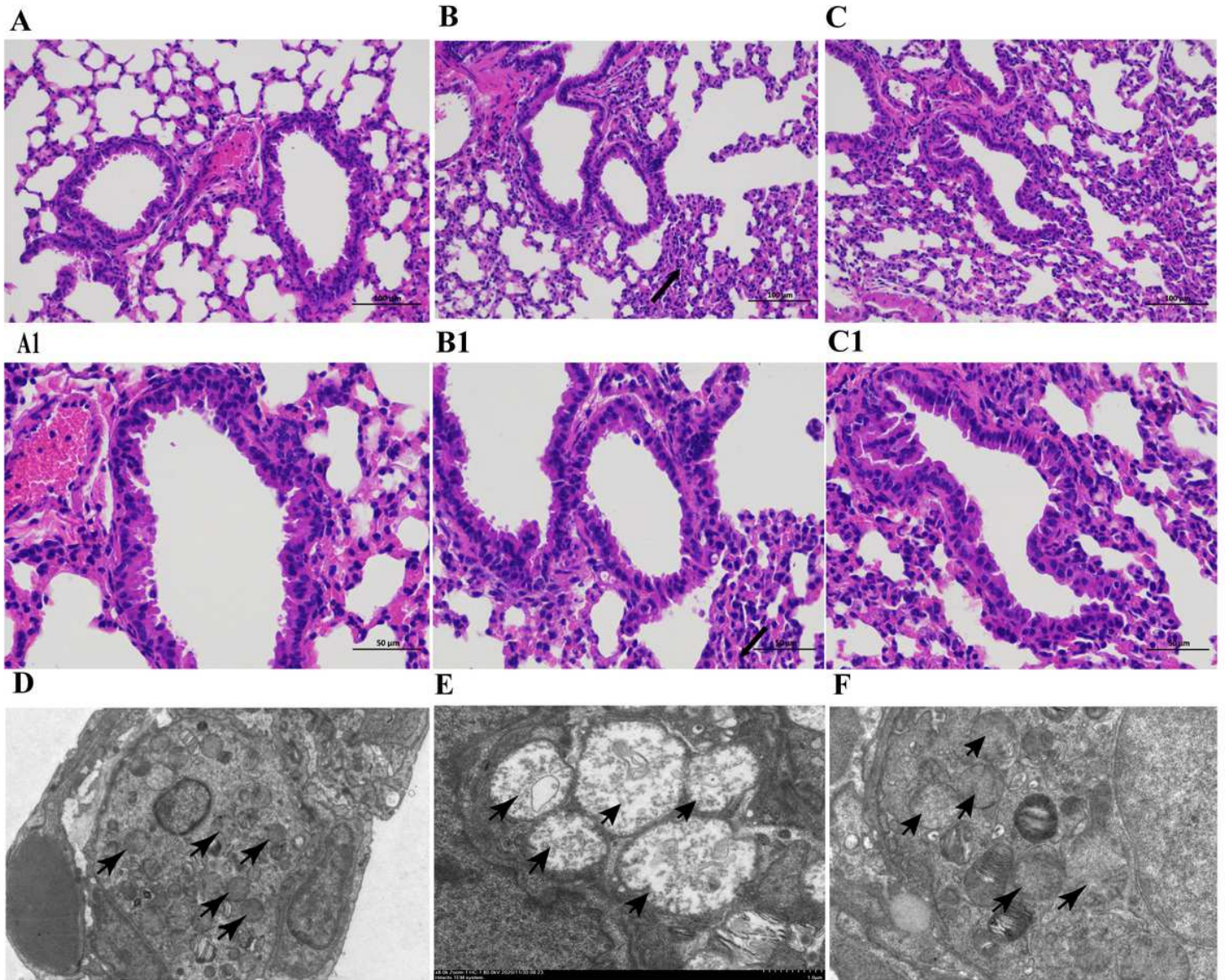524   #$P < 0.05$ vs model group; ##$P < 0.01$ vs model group.

Figures

Figure 1

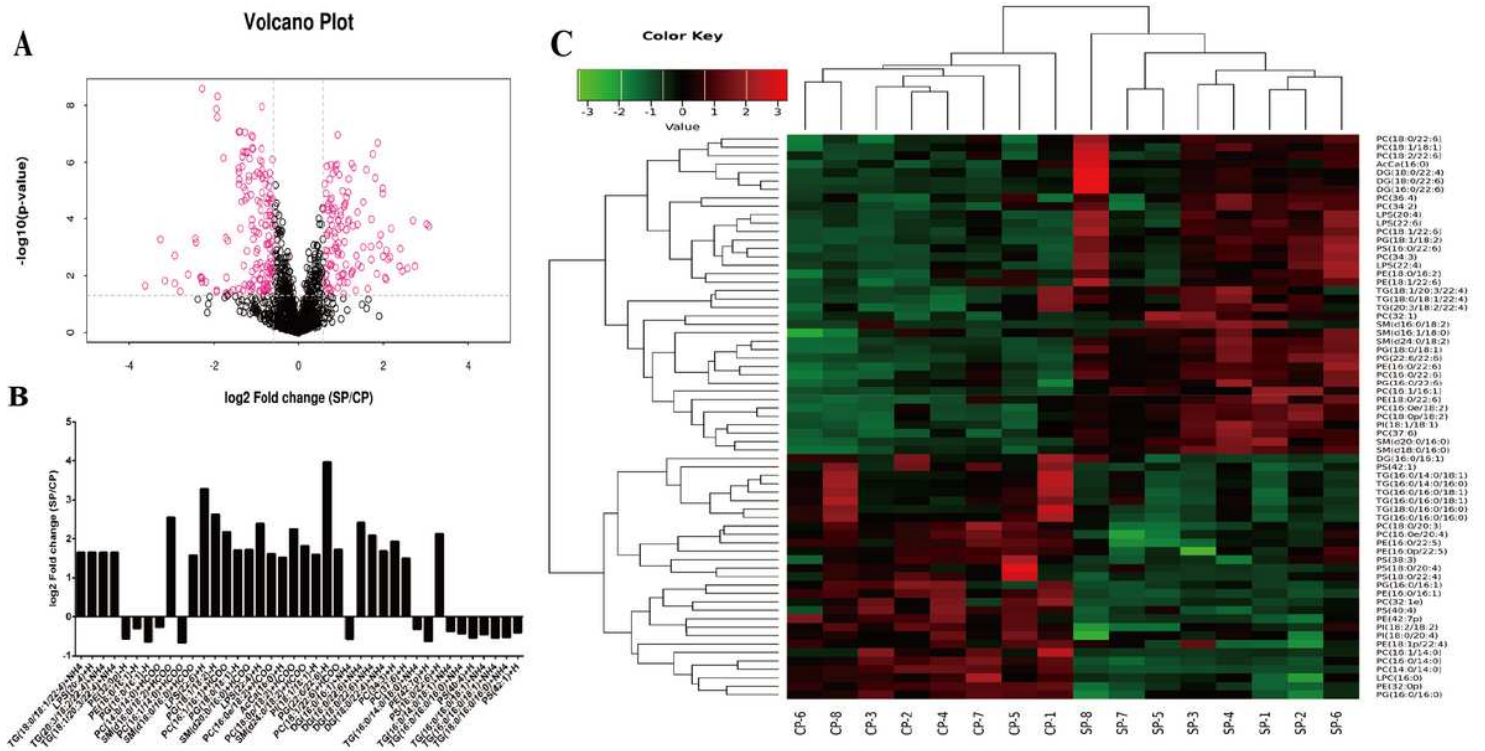Total ion chromatogram fingerprint of XJDHT formulae.

Figure 2

Survival curves were analyzed by log-rank (Mantel-Cox) test demonstrating an increase in median survival of 15 hours in the XJDHT treatment group (P<0.05).
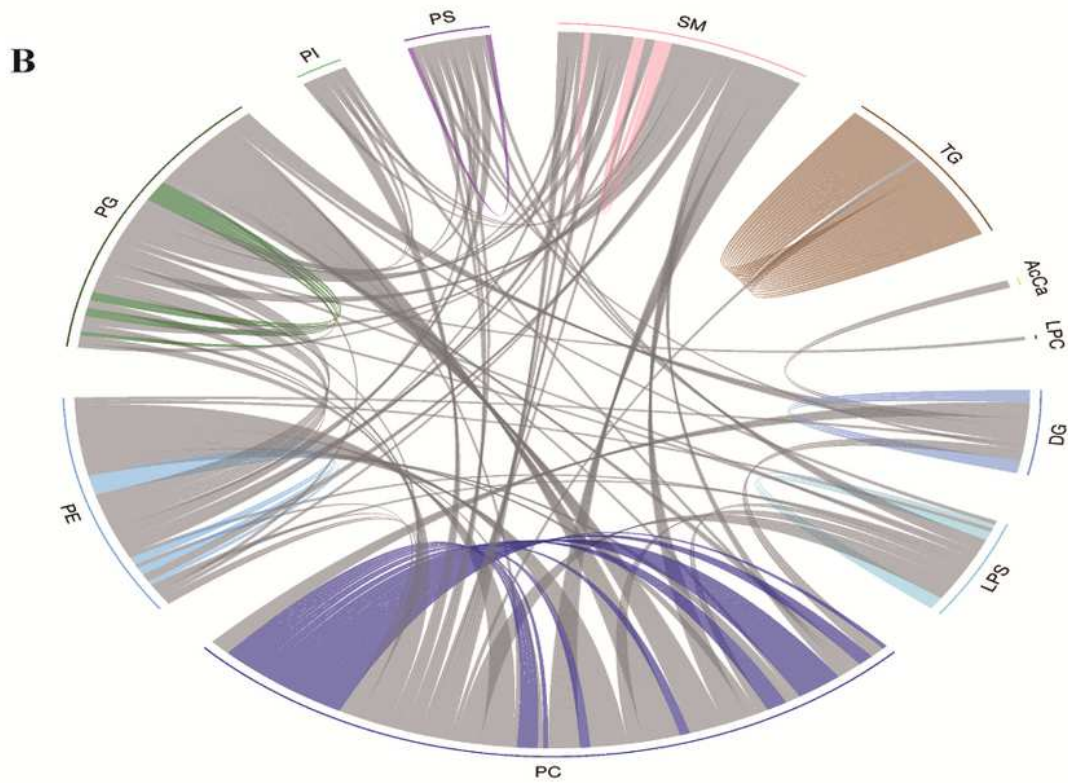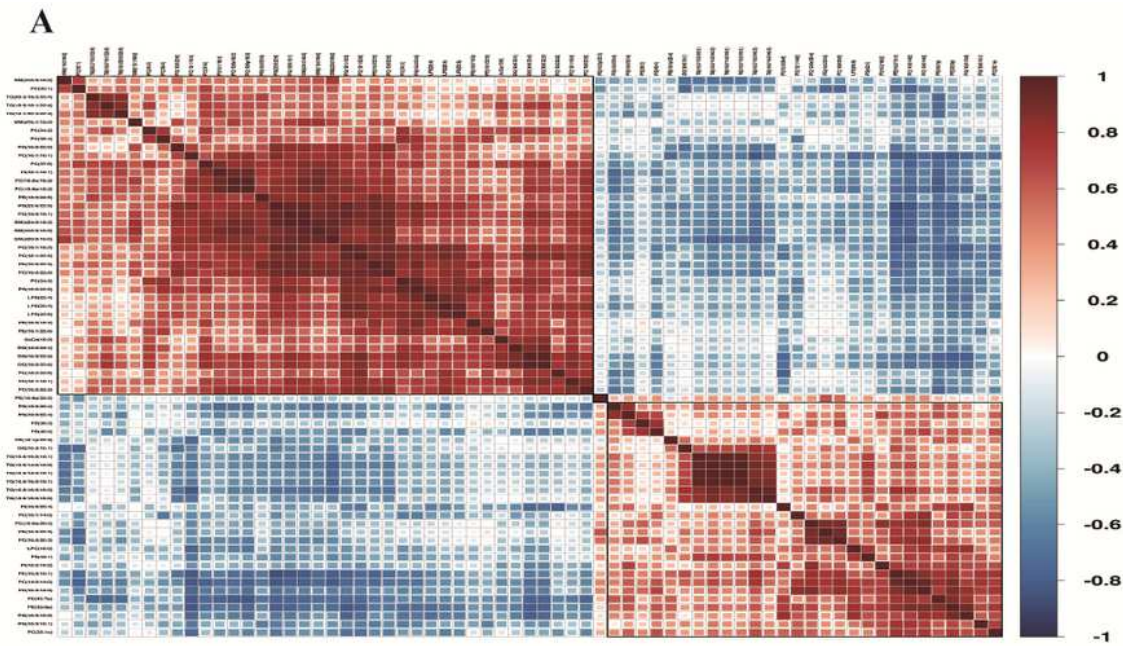
Figure 3

Histopathological changes of lung. (A-A1): Normal control group, no obvious abnormality in the structure of bronchus, the alveolar wall was composed of a single layer of epithelium, and the structure was clear; there was no obvious abnormality in the interstitium including connective tissue and blood vessels in the lung, and there was no obvious inflammatory change. (B-B1):Sepsis group, Mild to moderate alveolar wall thickening, black arrow indicates inflammatory cell infiltrates. No other obvious abnormalities were observed in the tissue. (C-C1): XJDHT treatment group, no obvious abnormality of bronchial structure in visual field, clear alveolar structure, No obvious inflammatory infiltration. (H&E × 200), Original magnification; × 400. Scale bar represents 50 μm. Normal control group (D): Mild mitochondrial swelling (black arrow). Sepsis group(E) Severe mitochondrial swelling (black arrow). XJDHT treatment group, Moderate mitochondrial swelling (black arrow).

Figure 4

(A-B): The composition of lipid classes in control group and sepsis group; C: The dynamic distribution range of lipid content of different groups; D: Lipid subgroup and lipid molecule count were based on the International Lipid Classification and Nomenclature Committee. Abscissa indicates lipid class was detected, Ordinate indicates lipid species.
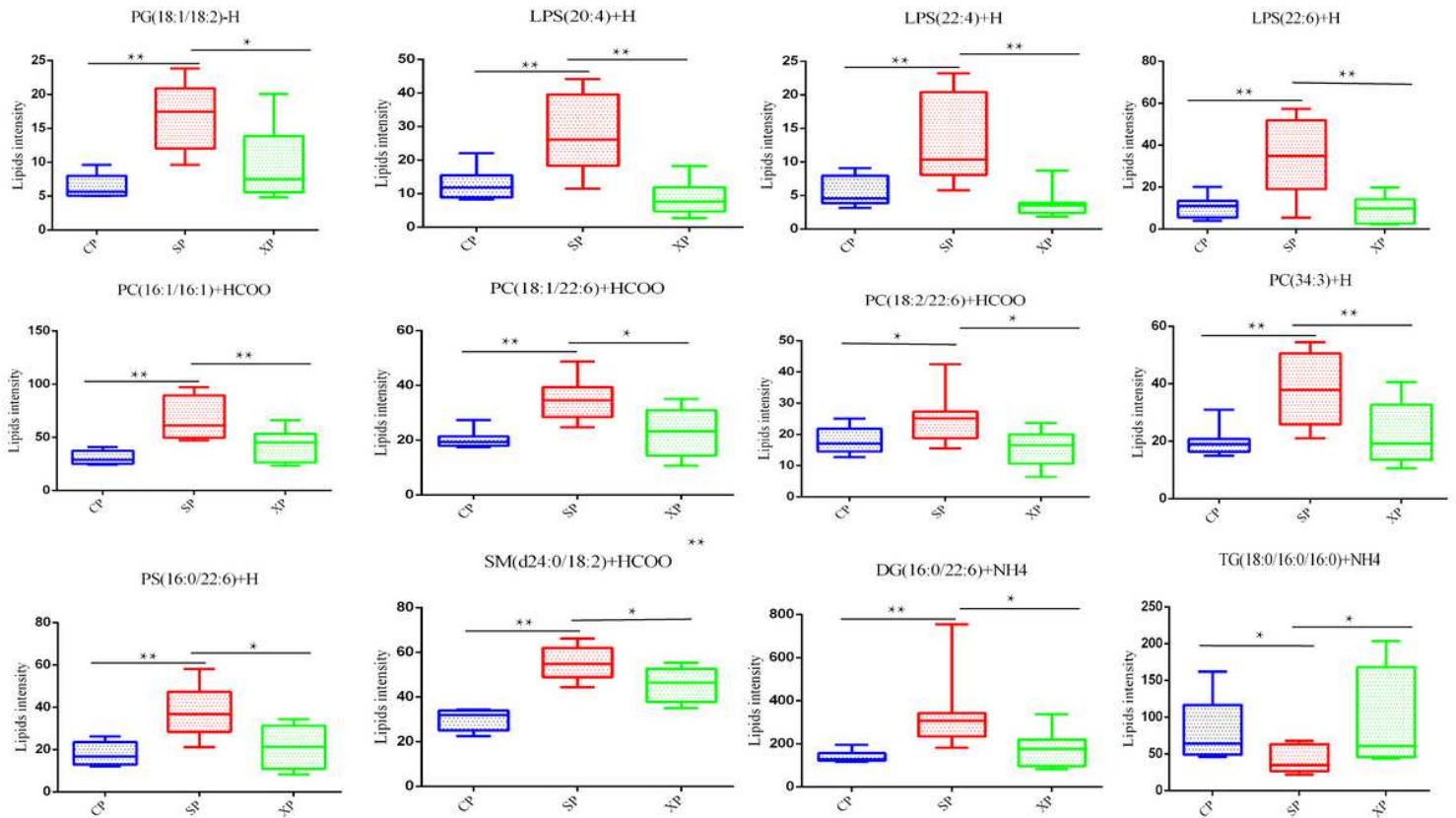
Figure 5

Principal component analysis of population samples in mice lung based on UHPLC-Orbitrap MS. (A) volcano plot of Sepsis-Control, red point represents the different lipids (FC > 2.0, P-value < 0.05); (B) Fold-change analysis of the different lipids between Sepsis-Control (CP-Control group, SP-sepsis group); (C) Clustering heat map of the lipids.

Figure 6

Lipomics analysis of the lung samples in septic mice. (A) Correlation clustering heat map of the lipids. Red means positive correlation, blue means negative correlation, color depth is related to the absolute value of correlation coefficient. The depth of color is proportional to the level of correlation coefficient. (B) Chord diagram of correlated lipid pairs in the lung of septic mice. The significant difference of lipid molecules was showed by a node around the circle plot and the lipid subclasses were demonstrated by

color coded. The color lines show the intra-class correlation, and the lines are the same color with the subclass. Dark gray lines represent interclass correlation.

Figure 7

Differential expression levels (mean) of 12 differential lipids in different groups. A comparison of the relative intensities of the potential biomarkers in the control, sepsis, XJDHT groups. *P < 0.05 vs control group; **P < 0.01 vs control group; #P < 0.05 vs model group; ##P < 0.01 vs model group.

Supplementary Files

This is a list of supplementary files associated with this preprint. Click to download.

- supplementaryinformation.pdf